

This pdf file consists of figures containing photographs, and their captions, scanned from:

EXAMPLES OF TECTONIC MECHANISMS FOR LOCAL CONTRACTION
AND EXHUMATION OF THE LEADING EDGE OF INDIA. SOUTHERN
TIBET (28-29 °N; 89-91 °E) AND NANGA PARBAT, PAKISTAN

by

Michael A. Edwards

A Dissertation

Submitted to the University at Albany, State University of New York

in Partial Fulfillment of

the Requirements for the Degree of

Doctor of Philosophy

College of Arts & Sciences

Department of Earth & Atmospheric Sciences

1998

Figure 2.5a



Figure 2.5a see caption on next page

Figure 2.5b

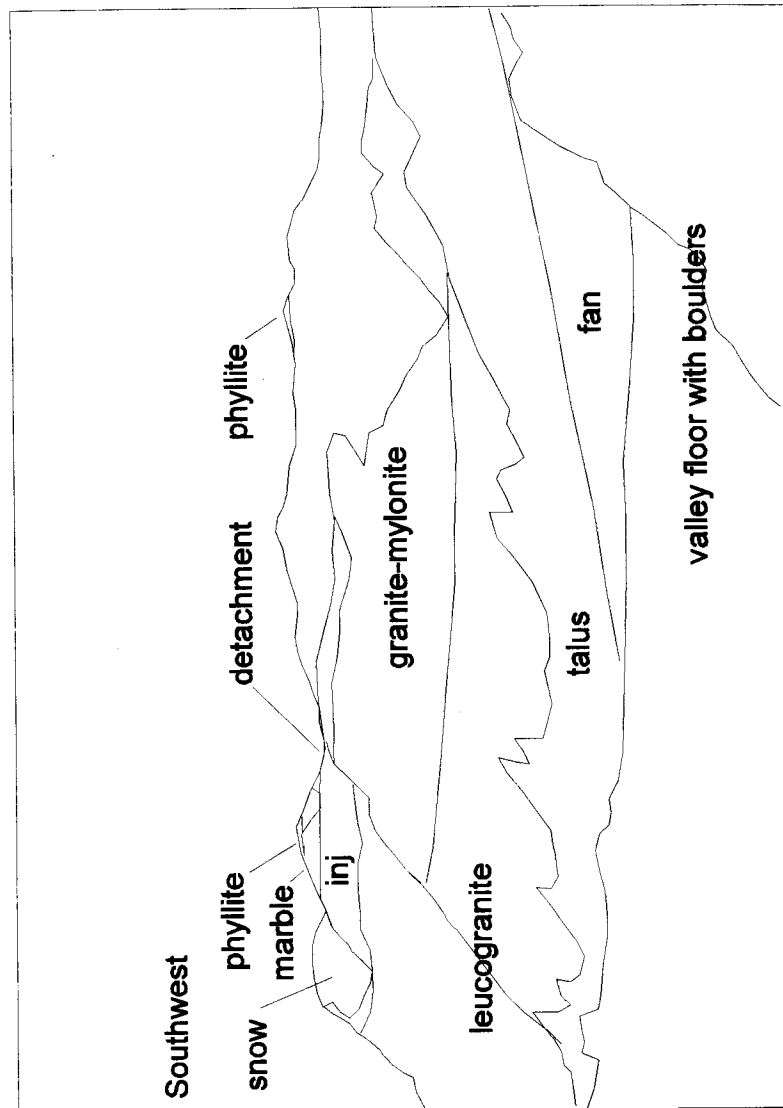


Figure 2.5b [a (previous page) & b] Photo and line drawing looking WSW from location 1 (fig. 2.3) at N end of Gonto La valley. Gonto La detachment is continuous line running across hillside, dipping approximately 10° N. Upper 300m up to detachment is granite-mylonite. Jagged cliffs in foreground are leucogranite of Khula Kangri pluton. Light and dark horizontal bands on peaks above detachment are gently north-dipping sequences of marble and phyllite respectively (described in text). Note thin outcrop of gently south dipping injection complex (inj) at location 3 (fig. 2.3), which illustrates gradual excision by both Gonto La detachment above, and pluton below. Towards south, injection complex layer systematically increases in both thickness and angle of dip (see description in text). DCF outcrops to right, outside field of view.

Figure 2.6a



Figure 2.6a see caption on next page

Figure 2.6b

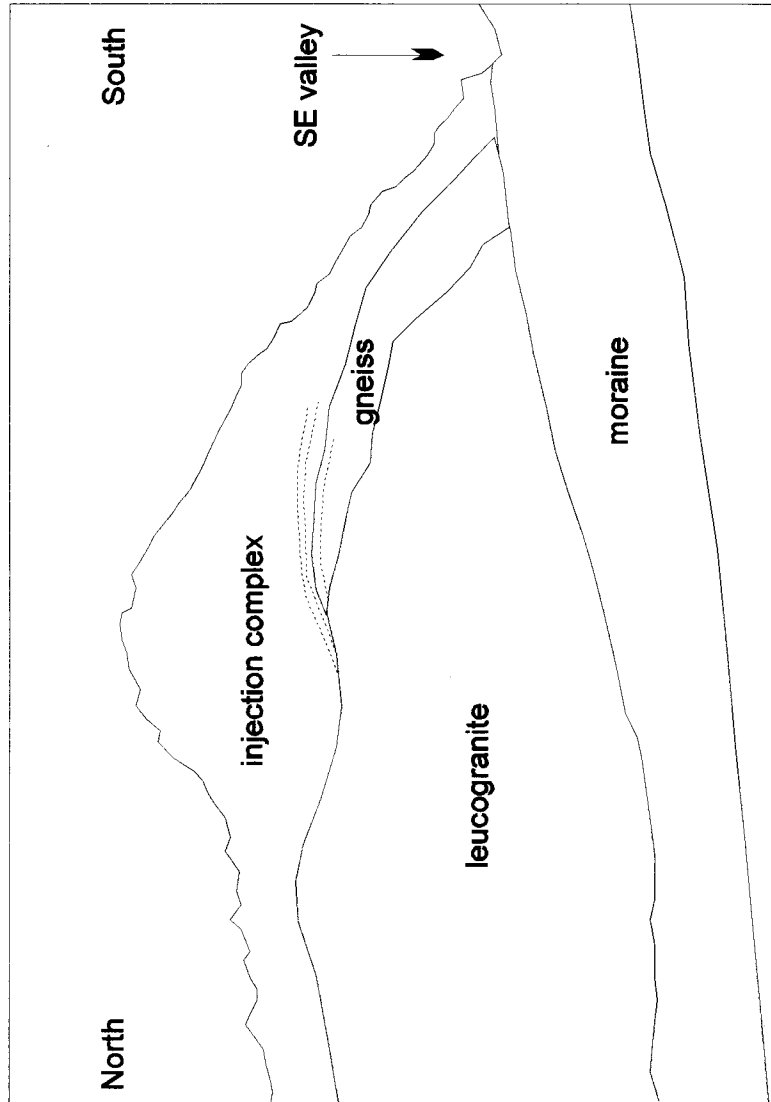


Figure 2.6b [a (previous page) & b] Photo and line drawing from location 4 (fig. 2.3) ~200m above valley floor on SW corner of main Gonto La valley looking across to entrance to SE valley (location 5, fig. 2.3). View shows intrusive southern contact of leucogranite of Khula Kangri pluton truncating the gneiss and, to left, cutting leucogranite sills which define macroscopic foliation. The leucogranite is unfoliated at this contact. This cross-cutting relationship requires that the granite post-dates development of the mylonite of the injection complex (see text). Mesozoic (?) phyllites, structurally above the injection complex, outcrop up the SE valley, out of view. The Gonto La detachment projects from where it last outcrops to the north (left) to above present erosion level. Apparent antiformal shape of foliation (dashed lines on line drawing) is distortion due to perspective.

Figure 2.7



Figure 2.7 Photomicrograph of mylonitic horizon of leucogranite (appendix B) from location 2 (fig. 2.3) in northern Gonto La valley illustrating typical sense of shear indicators observed. Cut perpendicular to foliation, parallel to lineation (350°); crossed polars. Side of image is ~ 4.0 mm. North is to base, south to top. Polycrystalline quartz and feldspar ribbon aggregates define S-surfaces. In lower centre, asymmetry of inclusion tails of feldspar grain and mica fish show sinistral sense of shear (top-to-north).

Figure 2.8

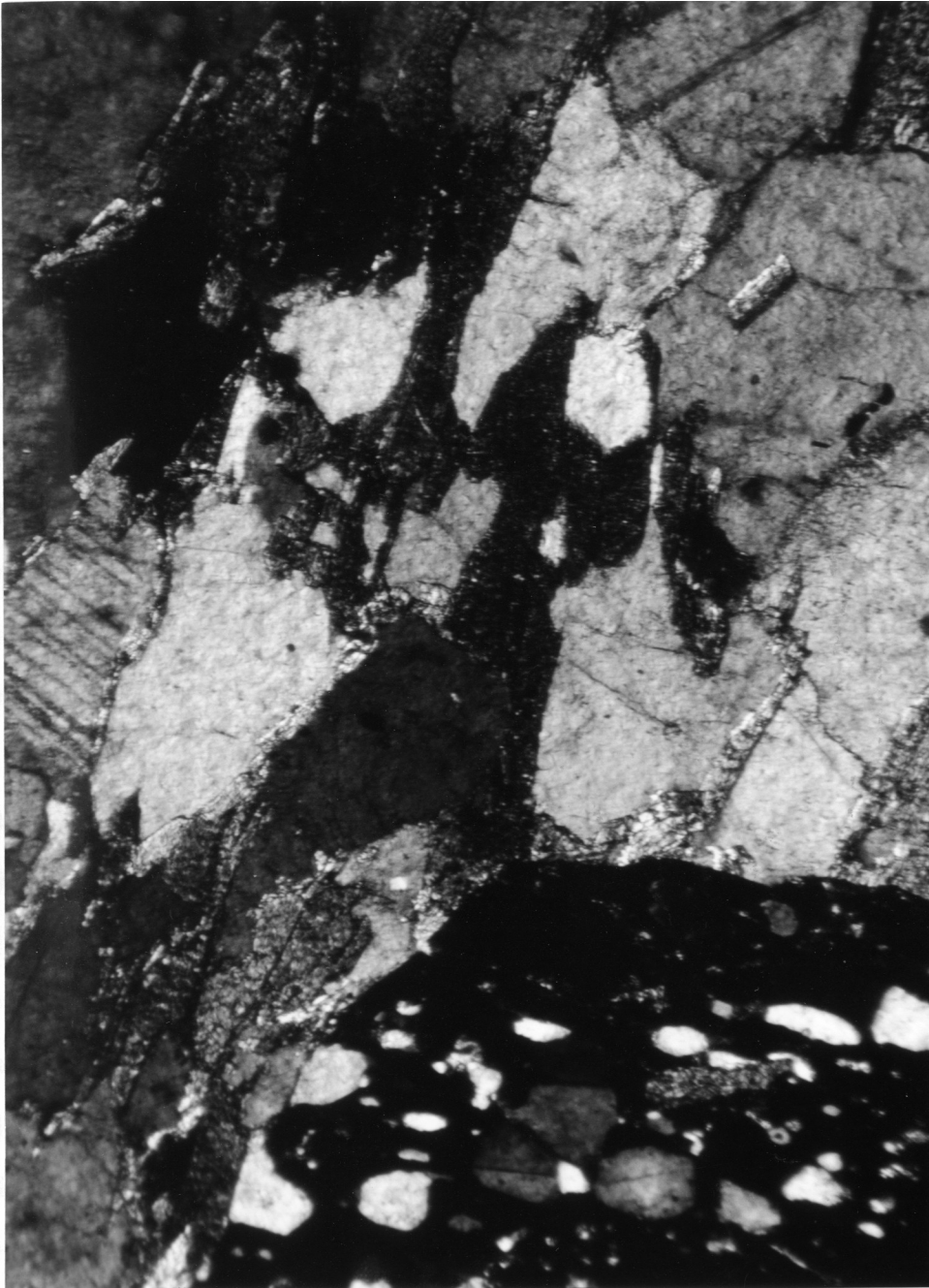


Figure 2.8 Photomicrograph of biotite-sillimanite gneiss (appendix B) near intrusive contact in southern Gonto La valley (location 5, fig. 2.3). Side of image is ~4.0mm. S_1 (in garnet grain) shows a foliation at a high angle to S_2 , the gneissic foliation. Crossed polars.

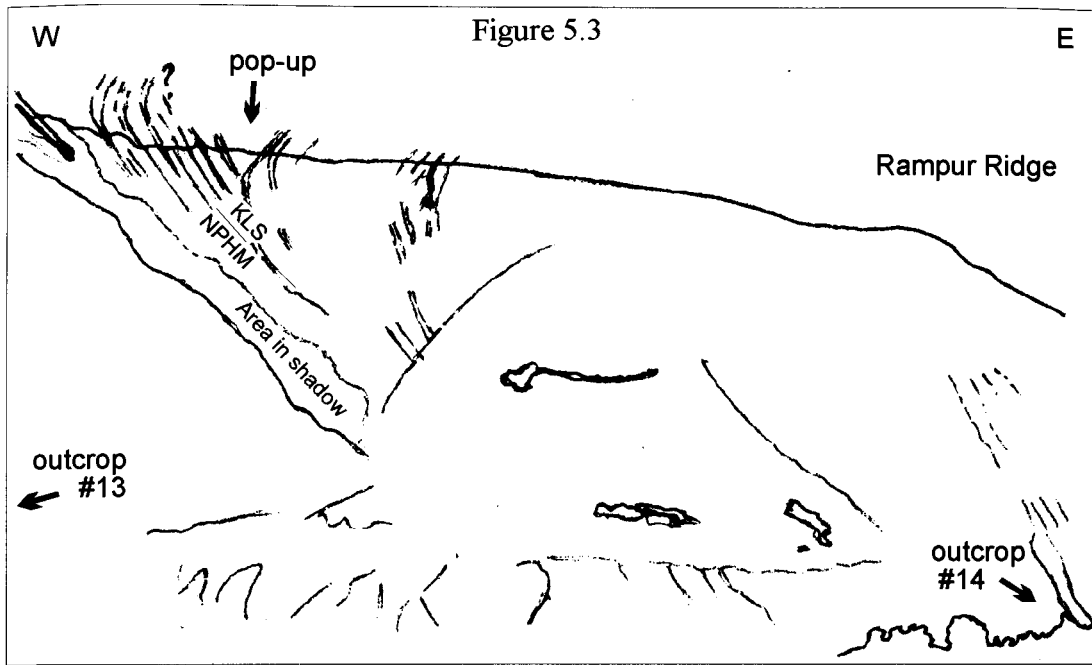


Figure 5.3 (field photo and line drawing). View to north of Rampur Ridge that forms easternmost portion of left bank of Lower Rupal Valley. Scattered fields and trees on level in foreground are ~2600 m in elevation. Central portion of Rampur Ridge is ~3700 m. Outcrop #14 is visible. Outcrop #13 is ~200 m beyond left edge of field of view. Contact between Kohistan Ladakh Series (KLS) and NPHM is present in hillside below Rampur Ridge and identified by pale brown east-dipping layers (labelled NPHM on line drawing) structurally below dark green layers (labelled KLS on line drawing). Note (1) local ~100 m wide pop-up structure and overturning of KLS layers east of pop-up. Photo 21/9/96 no.5.

Figure 5.4



Figure 5.4 Looking N. to left bank of Lower Rupal Valley. Cascade folding of mm-cm-10's cm layered garnetiferous metapelites interlayered with cm to 10's cm amphibolite and biotite schist. Trend is $\sim 005^{\circ}$ to 025° and axial planes dip $\sim 65-75^{\circ}$ W. Note overall monoclinial flexure is steep to left (west). Layers further steepen to left of field of view, and are overturned and truncated by a series of $40-80^{\circ}$ west-dipping, brittle fault sets of west-side up minor (centimetre to metre) displacement. Jeep track is cut into hillside directly below field of view. Thickest dark band in lower centre is ~ 0.75 m. Photo 21/9/96, no.3. View from right bank of Lower Rupal Valley.

Figure 5.5



Figure 5.5 Compositional layering within garnetiferous metapelites at outcrop #13, left bank of Lower Rupal Valley (c.f. fig 5.4). Note well-laminated quartzofeldspathic portions possibly suggesting high strain (c.f. fig. 5.8). Hammer for scale. Photo 6/7/95, no.5a

Figure 5.7



Figure 5.7 Looking S and upwards, on right bank of Lower Rupal Valley (few 10's m W of outcrop #50). Mitch Wemple standing on cascade folds within layered garnetiferous metapelites. Trend is $\sim 178^\circ - 015^\circ$ and axial planes dip $\sim 68^\circ$ W. Hinge lines plunge $\sim 38^\circ @ 005^\circ$. Note (1) prominent fold hinges in centre, and (2) crenulation intersection lineation developed below Mitch's left foot. Photo 21/9/96, no.4.

Figure 5.8

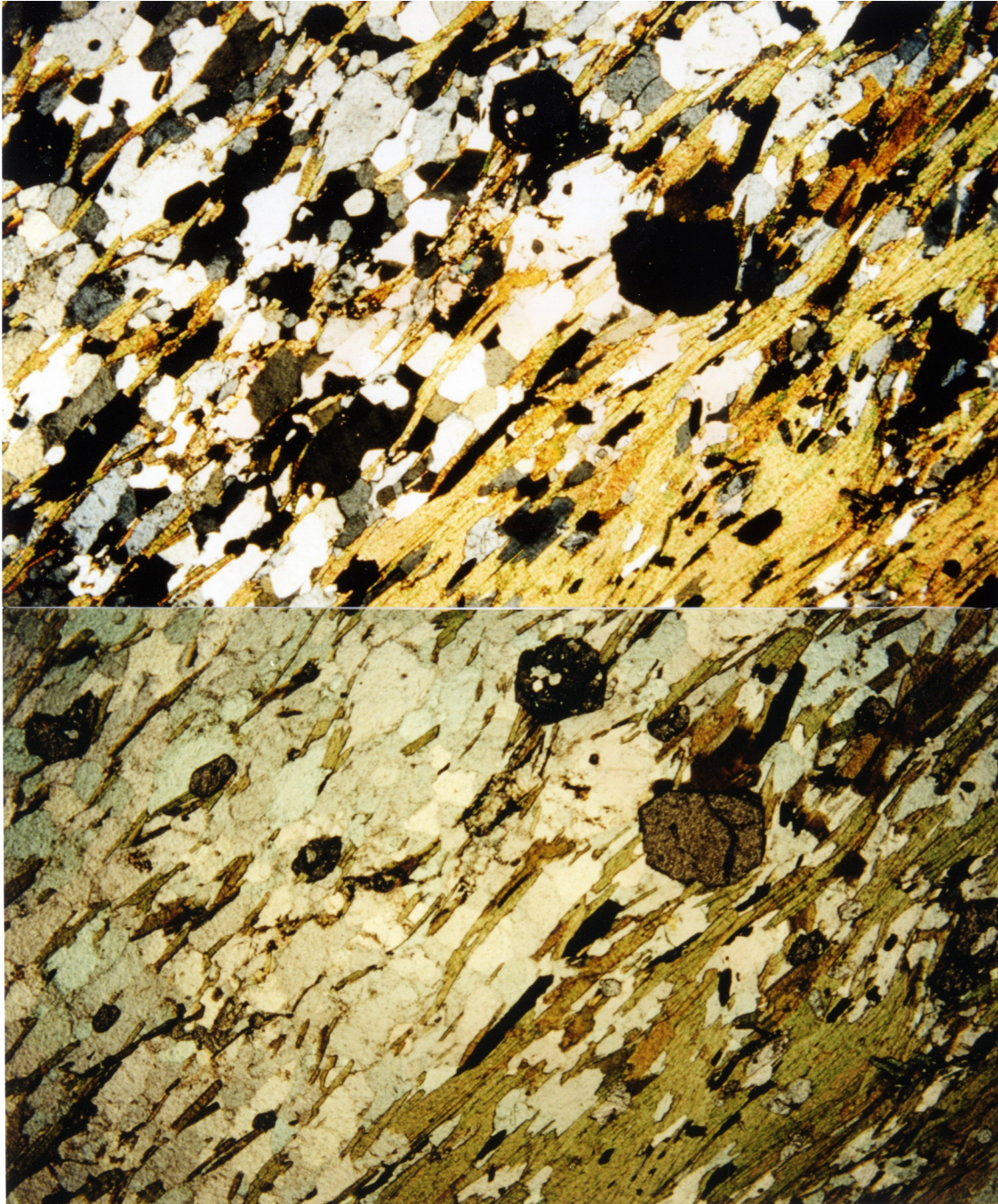


Figure 5.8 Optical photomicrographs (upper - crossed polars, lower - plane polarised light) of thin section 5/29F (cut from NE95/29-VI), garnet-biotite-amphibole schist from outcrop #13. Photo is taken with foliation oblique to horizontal to emphasise (1) proto-sedimentary layering (hornblende rich & poor portions) and (2) lattice preferred orientation in hornblende. See text for sense of shear discussion. South is to bottom left, north is to top right. Cut parallel with lineation ($20^\circ@005^\circ$), perpendicular to foliation ($010^\circ/85^\circ\text{E}$). Image base is 5.5 mm.

Figure 5.9

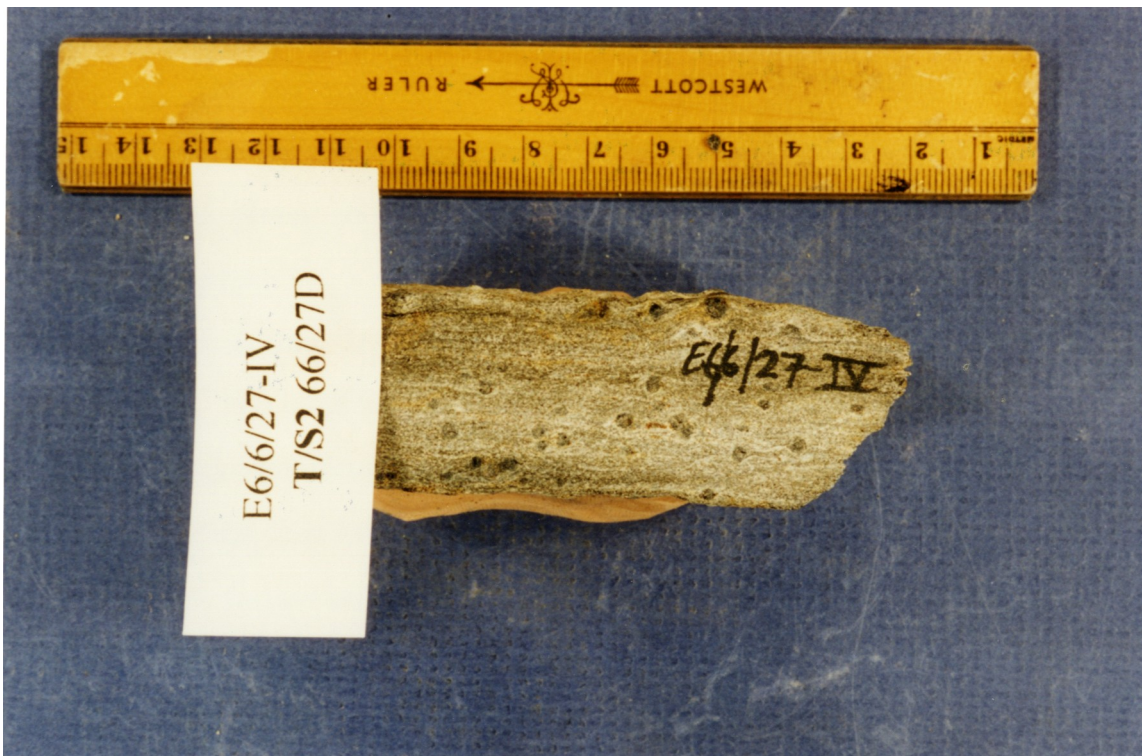


Figure 5.9 Sample E6/6/27-IV from near KLS/NPHM contact on left bank of E Astor Gorge. $170^{\circ}/89^{\circ}\text{E}$, $15^{\circ}@170^{\circ}$. Illustrates pressure shadow asymmetry in a garnetiferous metapelite. Sense of shear is dextral, consistent with fig. 5.10 (thin section 66/27D). This is typical for sense of shear observed in metasedimentary rocks along E. Astor Gorge.

Figure 5.10

Figure 5.10 (next page) Optical photomicrographs (upper - crossed polars, lower - plane polarised light) of thin section 66/27D, (cut from sample E6/6/27-IV). Illustrates pressure shadow asymmetry in a garnetiferous metapelite. Garnet shows good inclusion trails that suggest a rotation (in this case, clockwise i.e., dextral sense) of the garnet relative to the principal fabric defined by the micas (photomicrograph oriented with base of image approximately parallel to principal fabric). On all sides, the micas seem to bend around the garnet and there appears to be no post-kinematic growth. Other garnet porphyroblasts in this thin section are consistent. Sense of shear is dextral, consistent with other metasedimentary rocks along this part of E. Astor Gorge. Cut parallel with lineation ($15^\circ@170^\circ$), perpendicular to foliation ($170^\circ/89^\circ\text{E}$). South is on left. Base of image is 5.5 mm.

Figure 5.10

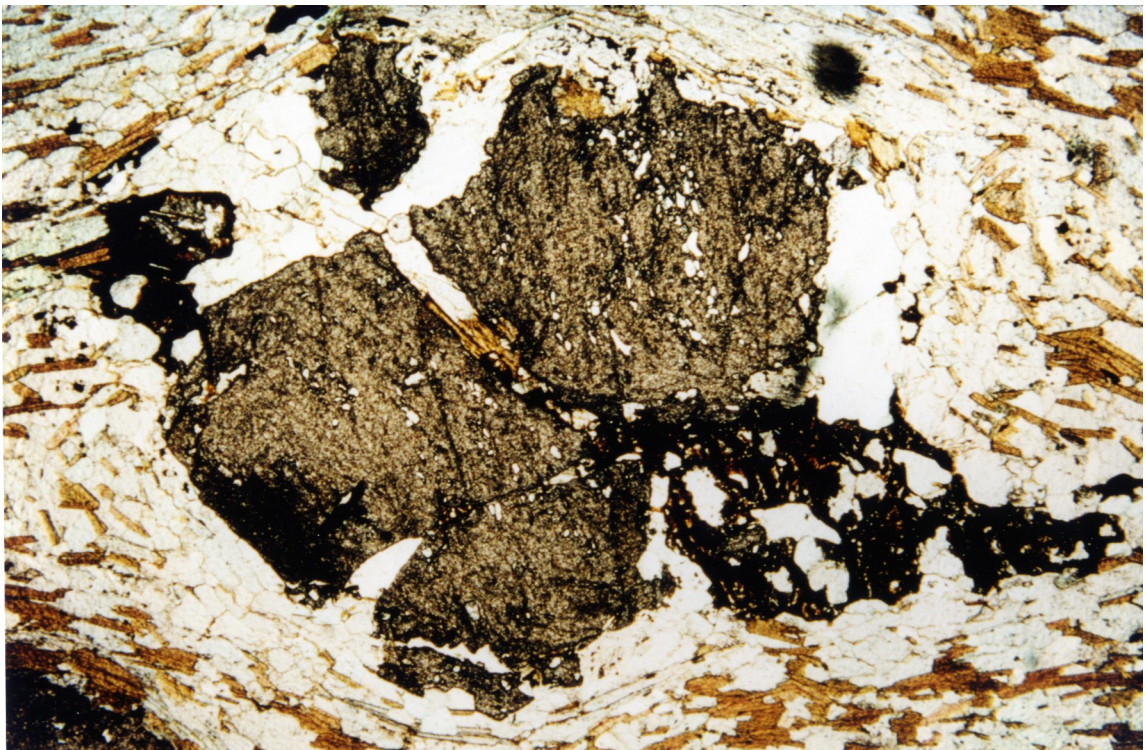
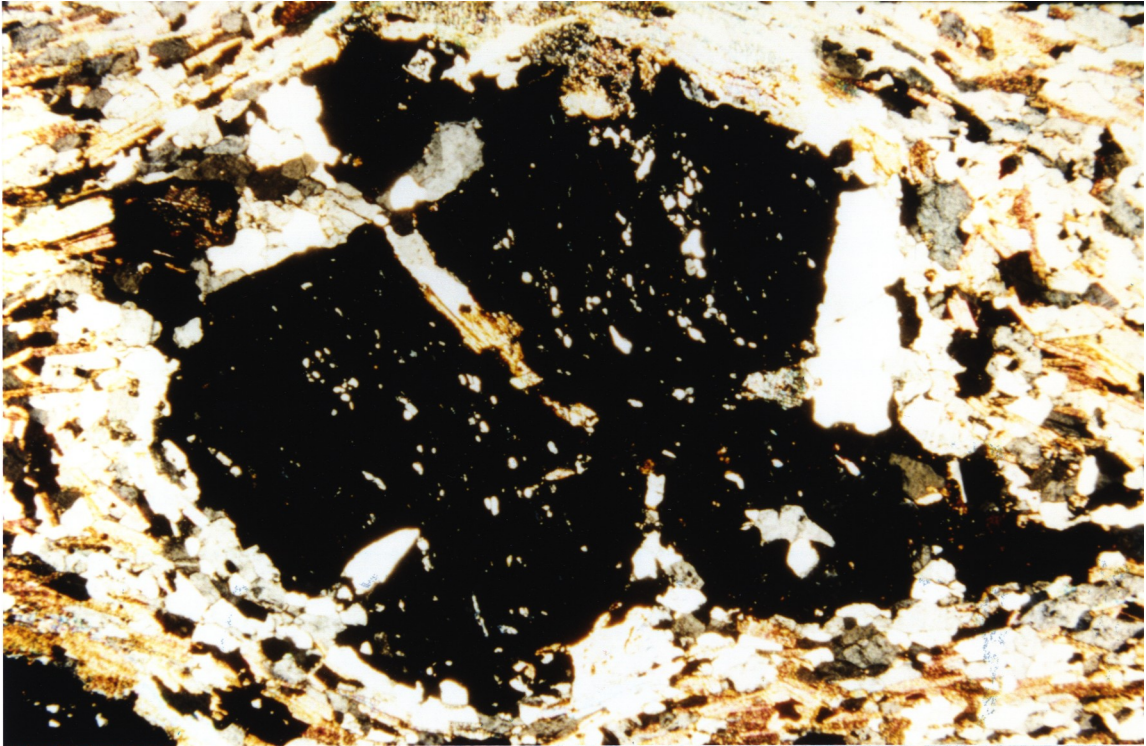


Figure 5.10 See previous page for figure caption.

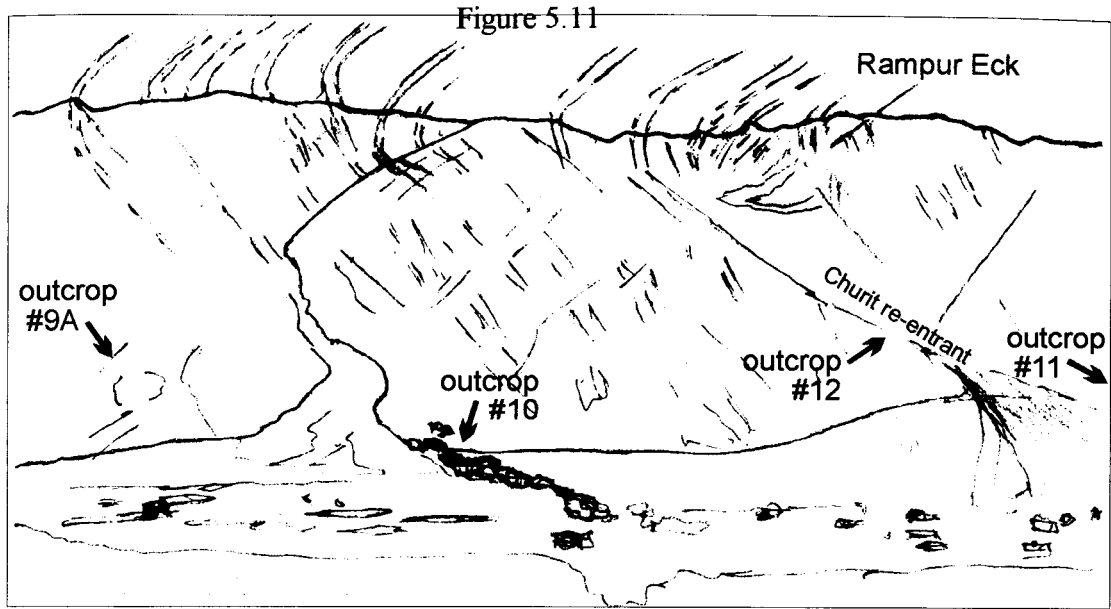


Figure 5.11 (field photo and line drawing). View to north of Churit Ridge that forms central portion of left bank of Lower Rupal Valley. Scattered low buildings and trees on level in foreground are Churit Village (2685m). Rampur Eck (west of Rampur Ridge) is 3884m. Outcrops #9A, #10, and #12 are visible. Churit re-entrant is marked by apparent closure of orange band and by fan descending to bottom right of field of view. Churit faults are distributed throughout re-entrant (see text). Travertine deposits of outcrop #10 coincide with freshwater spring and top of line of trees. Main layering above Churit is 70-89°E but appears less steep due to perspective. For discussion of steep/overtuned layers, see text. Photo 21/9/96 no.8.

Figure 5.12



Figure 5.12 Photo of quartzofeldspathic-biotite-amphibolite gneiss found as float from scree on eastern edge of fan flowing out of Churit re-entrant. Very high strain is more clearly seen in fig. 5.13 (below).

Figure 5.13



Figure 5.13 High strain zone near outcrop #70A, within a $\sim 60^\circ$ west-dipping sequence of amphibolites, marbles and quartzofeldspathic gneiss on right bank of Bulan Gah. East is to left of picture, west is to right (note that layering of NPHM rocks throughout Bulan Gah dip gently to steeply west). Metre-scale boudins of amphibolite gneiss suggest sinistral sense of shear based upon boudin asymmetry and pinch and swell morphology. Also note asymmetric pinching fold adjacent to left hand side of flat top of main boulder in foreground suggesting sinistral sense of shear (flat top of boulder is approximately 3m wide). Photo 9/10/96 no.2, ~ 1.5 km upstream (W) from #70.

Figure 5.14



Figure 5.14 Angel hair unit at outcrop #62 on Rama left bank. Foliation: $159^{\circ}/33^{\circ}\text{W}$, lineation: $7^{\circ}@332^{\circ}$. Very stretched mm-scale rods of quartz and feldspar (where $L \gg S$) define high strain zone. Note cm-scale compositional banding, mm-scale augen and rusty garnets. "Matrix" typically is greyish pink. Lens cap for scale. Photo 7/10/96 no.1.

Figure 5.15



Figure 5.15 Optical photomicrograph of thin section 610/10A, (cut from sample E6/10/10-I, angel hair unit, ~750 m east of outcrop #73 on Dichil Gah left bank. 016°/53°W, 32°N-pitch). Illustrates likely tectonic grain size reduction based upon bimodal grain size distribution into ~300 μ m thick monomineralic quartz ribbons, and ribbons of very fine-grained (50-200 μ m) quartz and feldspar. Larger feldspar grains show suturing of margins to give partial core and mantle texture (not visible in figure). Sense of shear indicators are poorly developed both in figure and elsewhere in thin section. Left lateral is suggested by asymmetry of strain shadows and stepping of ribbons and trails associated with garnets, and slight development of oblique grains in lower part of picture. Cut parallel with lineation, perpendicular to foliation. South is on left. Base of image is 5.5 mm. Crossed polars.

Figure 5.16



Figure 5.16 Sample NE95/29-III, highly-strained garnet-biotite-quartz-feldspathic gneiss, immediately east of outcrop #12 ($020^{\circ}/40^{\circ}\text{W}$, 20° to N). Thin section (T/S2 5/29C - not shown) illustrates clear dextral shear sense based upon (1) oblique foliation of fine-grained component ($\sim 50\text{-}100\mu\text{m}$), (2) tail asymmetry and strain shadows in quartz and feldspar augen ($0.5\text{-}1.5\mu\text{m}$). (3) S-shapes in $100\text{-}300\mu\text{m}$ quartz ribbons, locally bent & thinned at stress contacts ("corners") of clast margins, and (4) mica fish.

Figure 5.17

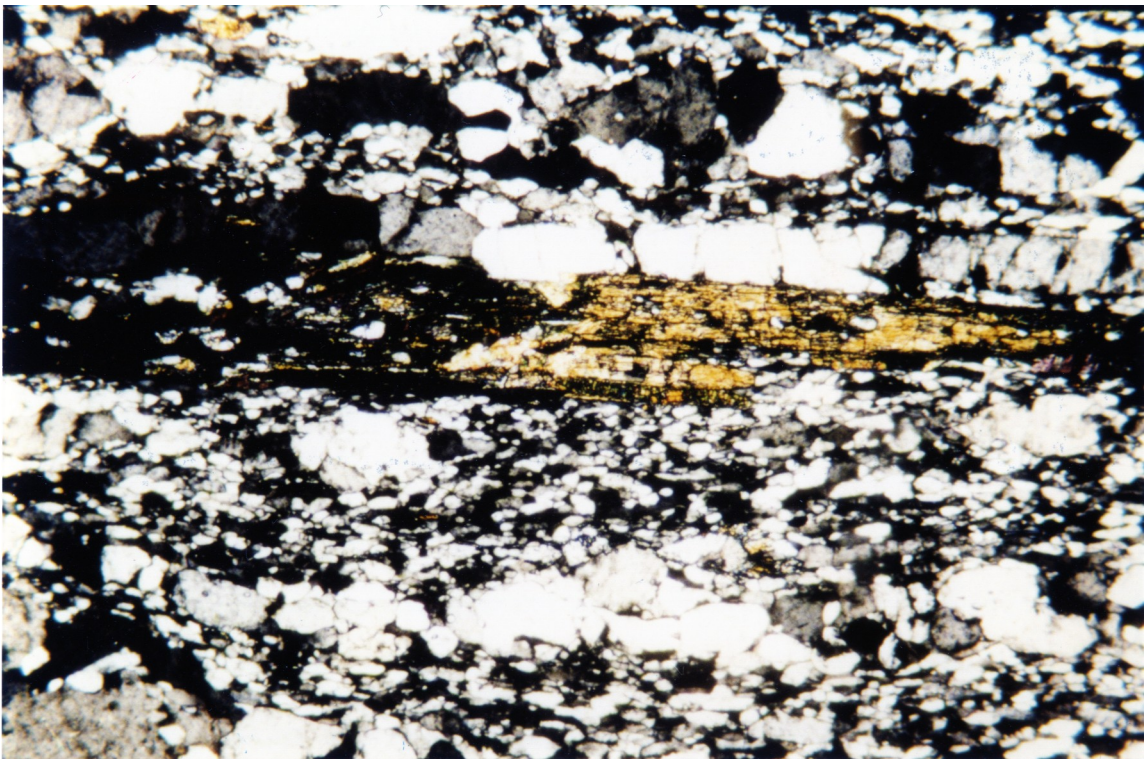


Figure 5.17 Optical photomicrograph of thin section 5/29D (cut from sample NE95/29-IV), fine-grained (50-100 μ m) L>>S granitic orthogneiss from west side of Churit re-entrant, ~50 m east of outcrop #12. Conditions of deformation are indicated by (1) C-surface parallel ribbons of quartz with even thickness (200-200 μ m), (2) ~300 μ m thick biotite grain that defines C-surface, (3) core and mantle appearance of certain feldspars (clearly seen in top left of photo) and (4) generally homogeneous flattening of <100 μ m quartz groundmass (below biotite grain). Dextral sense of shear. Cut parallel with lineation (10°@359), perpendicular to foliation (180°/70°W). South is on left. Base of image is 5.5 mm and parallel with main fabric. Crossed polars.

Figure 5.18



Figure 5.18 Sample NE95/29-II, fine-grained L>>S garnet biotite quartzofeldspathic gneiss from outcrop #12 on west side of Churit re-entrant. Note blebs of quartz and feldspar stretched out into striking 1-3 mm thick rods indicating very high strain. Garnets (~2-5 mm) and quartz and feldspar augen show sigmoidal and deltoidal trails.

Figure 5.19



Figure 5.19 Optical photomicrograph of thin section 5/29B (cut from sample NE95/29-II), fine-grained (50-100 μ m) L>>S garnet biotite quartzofeldspathic gneiss from outcrop #12, west of Churit re-entrant. Prominent 0.25-0.75 mm monomineralic quartz ribbon suggests dextral sense of shear, as does oblique foliation (more conspicuous below ribbon). Dextral shear sense is also shown by mica fish, strain shadows on garnet and hornblende grains and tails from feldspar augen, elsewhere in thin section (not shown). Very finely sutured grain margins of large (1-3 mm) augen and fine (50-100 μ m) groundmass indicate extensive grain boundary migration. Cut parallel with lineation (10°@005°), perpendicular to foliation (005°/89°W). South is on left. Base of image is 5.5 mm and parallel with main fabric. Crossed polars.

Figure 5.20

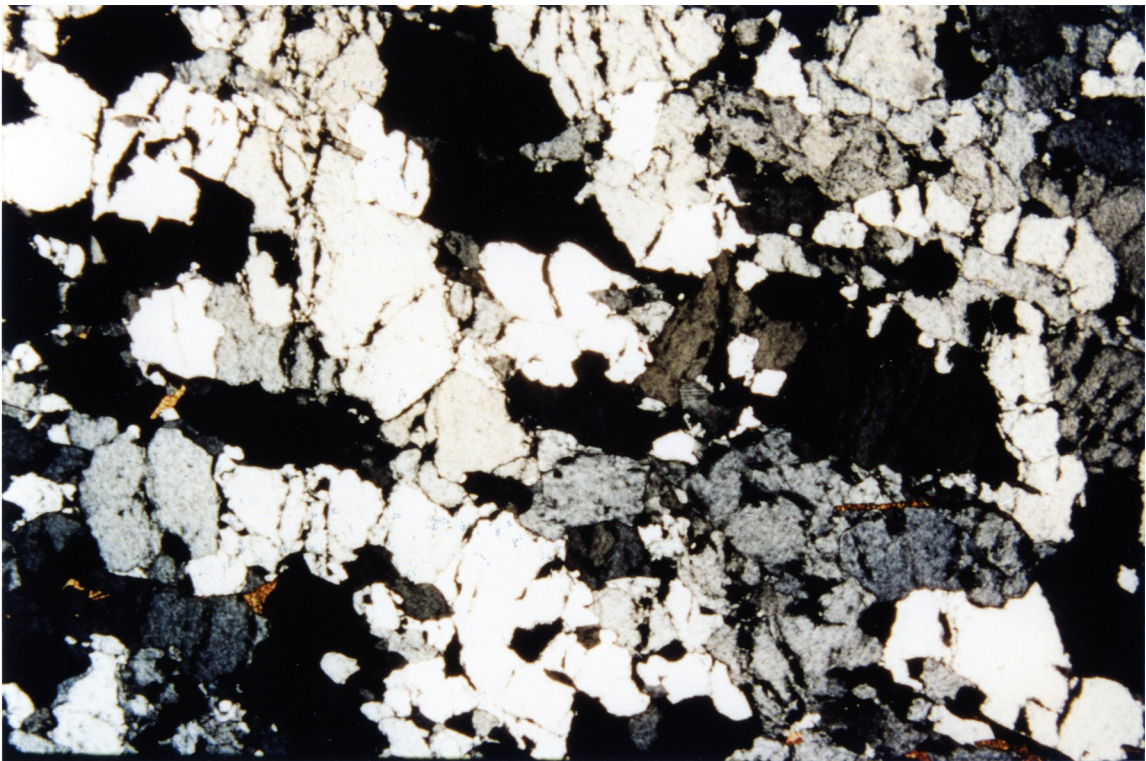


Figure 5.20 Optical photomicrograph of thin section 5/29A (cut from sample NE95/29-I, 020°/80°E; 20°N). Note generally "unstrained" appearance. Feldspars are clean; little to no significant patchy/undulose extinction. Some suturing of grain boundaries indicating limited operation of grain boundary migration. Note feldspars have "pitted" appearance. Large cracks in feldspars are not associated with extinction angle variation, suggesting lattice continuity. Cracks are inferred to be growth features (see text for discussion). Cut parallel with lineation, perpendicular to foliation. South is on left. Base of image is 5.5 mm and parallel with main fabric. Crossed polars.

Figure 5.21



Figure 5.21 Migmatite-rich portion of garnet-pelitic gneiss within general cover sequences (outcrop #69 - west of Churit Fault Zone in Ghurikot main valley). South is on left, view is from above. Foliation: $160^{\circ}/65^{\circ}\text{W}$; lineation: 2°N . Based upon stepping directions of augen and leucosome tails, sense of shear is dextral, however, 1-2 cm long C' -surfaces (below arrow to top left of compass) trending NNE-SSW suggest sinistral sense of shear. Compass for scale. Photo 8/10/96, no.4.

Figure 5.22



Figure 5.22 Field photo looking north to left bank of main valley in Ghurikot Gah (near outcrop #68). Illustrates local buckling and fracturing associated with a zone of E-vergent displacement within Churit Fault zone. Note moderate west dip of overall gneissic layering and area in foreground where jointing is antiformally folded. Tree in top right of photo is about 8 m high. Photo 8/10/96, no.3.

Figure 5.24



Figure 5.24 Field photo at outcrop #14 showing hornblende needles post-kinematically grown on foliation plane of very fine grained actinolite/tremolite schist (revealed by W.S.F. Kidd). Very continuous, even, m-cm compositional layering (not seen) suggests original metamorphism associated with high strain (see text for discussion). Rock is part of Kohistan Ladakh series (KLS). Photo 5/7/96, no.4.

Figure 5.26



Figure 5.26 Field photo looking north to left bank of main valley in Ghurikot Gah (near outcrop #66). Illustrates local folding associated with regional overturning of SE NPHM layering to W-dipping. Outcrop in bottom right is approximately 10 m high. Photo 8/10/96, no.1.

Figure 5.27



Figure 5.27 (field photo). View to west and upward to Bulan Peak (4915 m) showing ~500m (structural thickness) of NPHM metasedimentary rocks - schists and gneisses interlayered with marbles and amphibolites (recognisable as continuous black bands). Approximately 40°W true dip of foliation not clear due to perspective (see fig. 5.28). Photo 29/9/96 no.4. View from left bank of Astor Valley.

Figure 5.28



Figure 5.28 (field photo). Looking N. to left bank of Chuggam Gah, in Rattu area (3000-3500m main ridge in foreground). Small top of ridge just visible in centre of depth of field is Rampur Ridge (3884m). Bulan peak (4915m) clearly visible in distance. Crop fields are at ~2500m). In all visible portions of ridges, W-dipping (overturned) compositionally layered NPHM metasedimentary sequence is visible. c.f. fig. 5.28, Photo 24/9/96, no.2.

Figure 5.31A

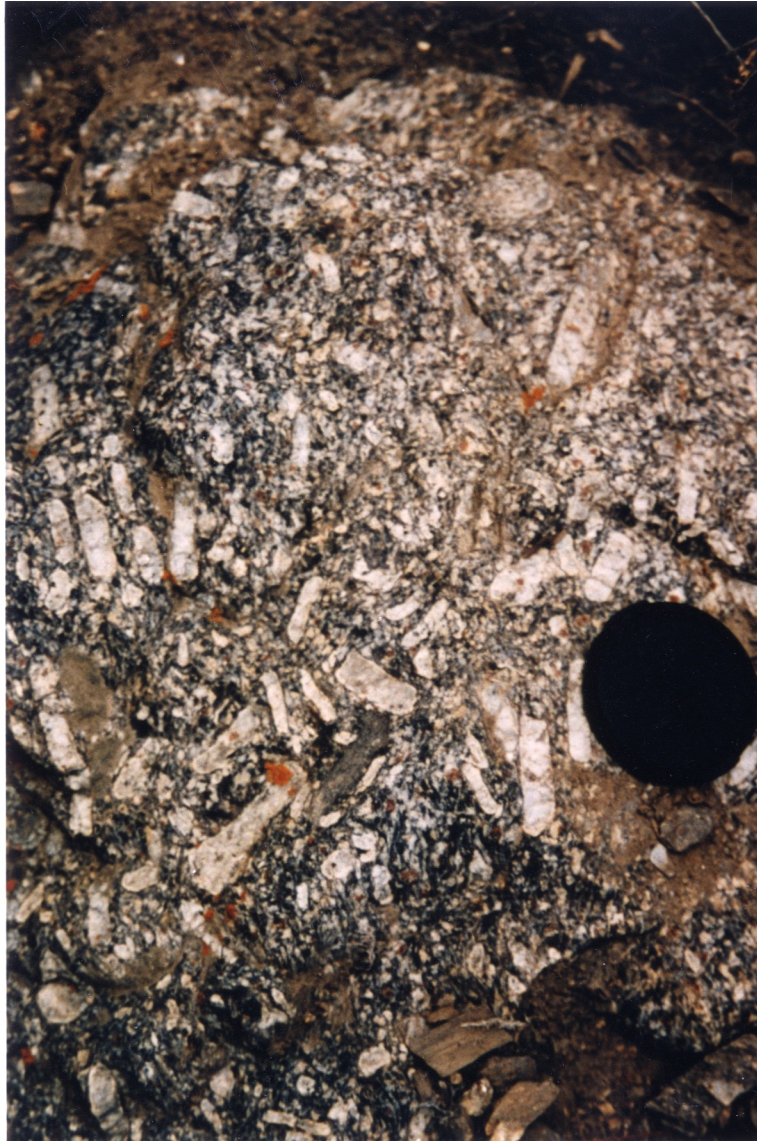


Figure 5.31A Lath unit outcropping on left bank of Rama Valley, ~300m east of outcrop #64. Note very disordered fabric picked out by generally non-preferred orientation of 1-4 cm laths of feldspar within biotite, garnet & quartzofeldspathic matrix. c.f. fig. 5.31B, taken ~10 metres nearby. Lens cap for scale. Photo 7/10/96 no.7.

Figure 5.31B



Figure 5.31B Lath unit outcropping on left bank of Rama Valley, ~300m east of outcrop #64. Indicates spectacular fabric gradient; portions with apparently greater shortening are visibly accompanied by change in foliation direction. Note foliation is highly variable and lineation only locally present. c.f. fig. 5.31A, taken ~10 metres nearby. Lens cap (55 mm) for scale. Photo 7/10/96 no.13..

Figure 5.32

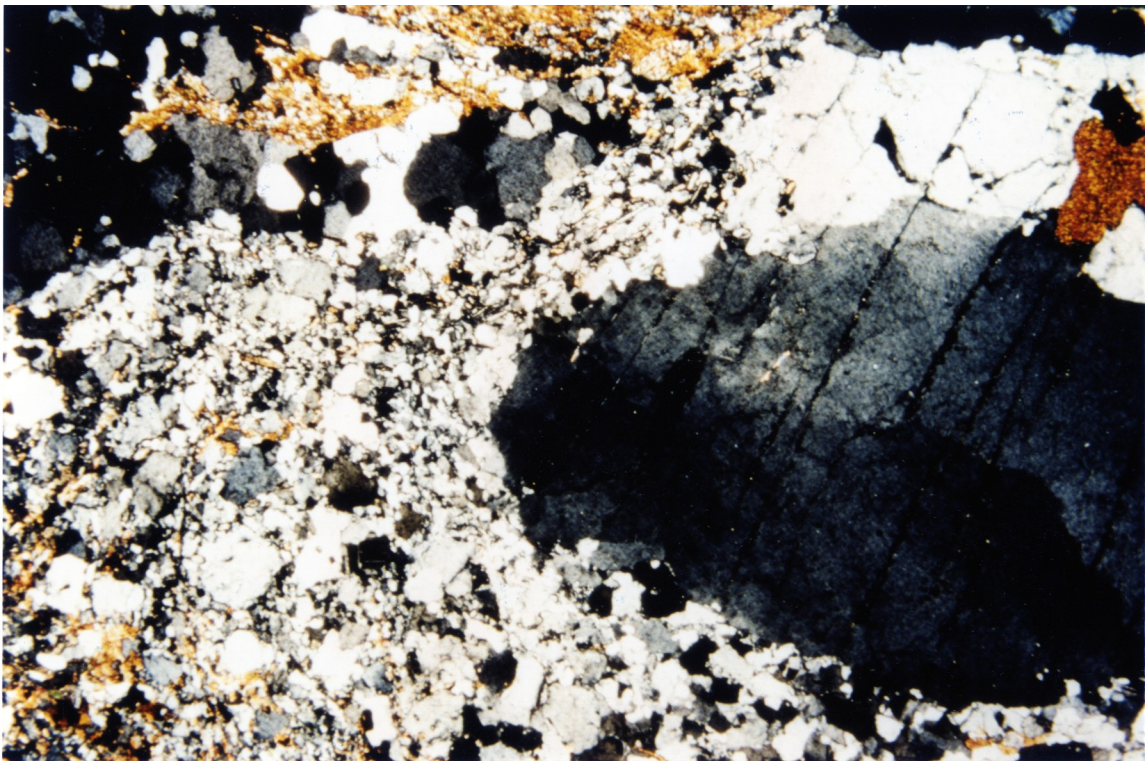


Figure 5.32 Optical photomicrograph of thin section AS/E, (cut from sample of same name, lath unit ~200m east of outcrop #71, on Astor Gorge left bank. 011°/43°W, 12°N-pitch). In upper left portion, 0.25-0.75 mm monomineralic quartz ribbon is typical appearance of quartz rich part of fine grained augen tail. Very finely sutured grain margins of large (>3 mm) feldspar clast and fine (50-150 μm) groundmass indicate extensive grain boundary migration recrystallisation. Not oriented. No sense of shear. Base of image is 5.5 mm long. Crossed polars.

Figure 5.34

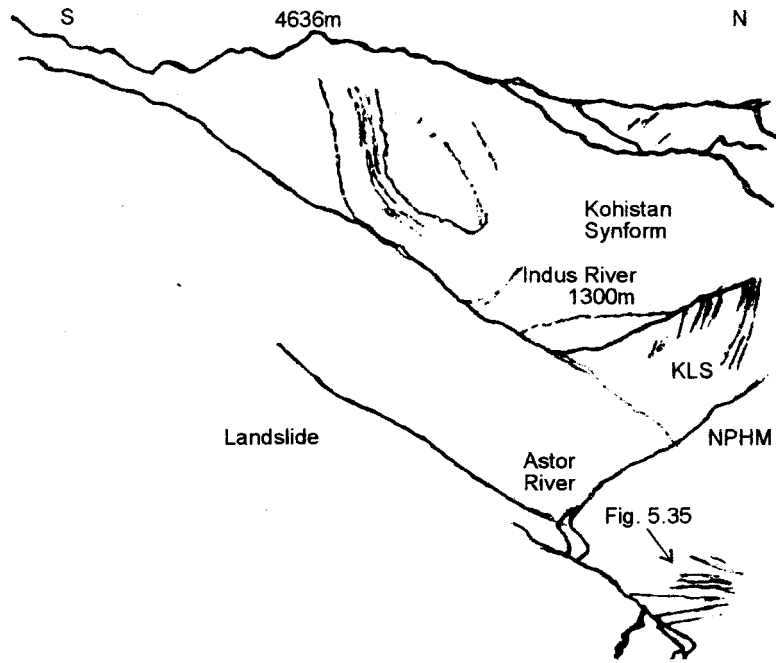


Figure 5.34 (field photo and line drawing). View to W over Indus River valley to Kohistan synform. Note contrast in NE dipping KLS layering and ~W dip of NPHM layering. Width of view ~2 km (foreground). Photo 6/7/96 no.0.

Figure 5.37



Figure 5.37 Field photo of Iskere gneiss outcropping along left bank of Astor Gorge. Note characteristic finely foliated ($023^{\circ}/83^{\circ}W$, $22^{\circ}@346^{\circ}$) grey granitic orthogneiss clearly cross-cut by migmatitic bodies (includes leucosome and melanosome). In photo, migmatitic bodies are isoclinally folded and sub-parallel to main foliation. Also common, however, are migmatitic bodies cross-cutting at high angles. Photo 10/10/96 no.10.

Figure 5.40A



Figure 5.40A Migmatite-garnet-pelitic gneiss at foot of Dichil Pass trail, ~200m below outcrop # 72 (Foliation: $007^{\circ}/89^{\circ}W$, hinge intersection lineation $25^{\circ}@007^{\circ}$). Note leucosome portion is isoclinally folded and lacks a strong melanosome. Swiss knife for scale. Photo 10/10/96 no.2.

Figure 5.40B



Figure 5.40B Cascade / parasitic folding within well-stretched amphibolite interlayered with migmatite-garnet-pelitic gneiss. Elsewhere (in large isoclinal hinge sections) amphibolite is seen to cross-cut migmatised gneissic foliation. Note crenulation intersection lineation clearly developed beside compass. Foot of Dichil Pass trail, ~200m below outcrop # 72 (hinge lineation $22^{\circ}@011^{\circ}$). Compass for scale. Photo 10/10/96 no.6.

Figure 5.42

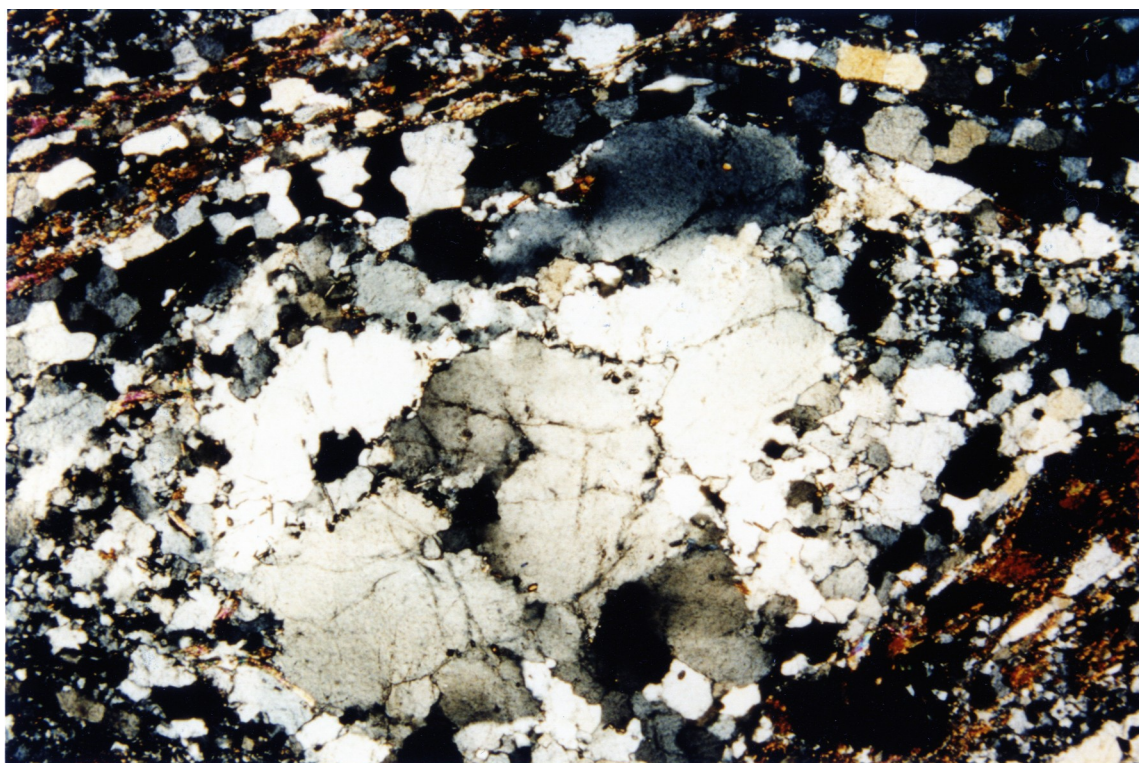


Figure 5.42 Optical photomicrograph of thin section 66/27E (cut from sample E6/6/27-V, not shown), deformed portion of lath unit on eastern Astor Gorge left bank, ~300m W of outcrop #71. Conditions of deformation are indicated by (1) C-surface parallel ribbons of quartz with even thickness (200-400 μm), (2) C-surface defined 100-200 μm thick biotite grain, (3) >3 mm feldspar clast with sutured internal grain boundaries indicating onset of grain boundary migration and beginnings of core and mantle texture within grain. Grain boundary migration and wholesale grain size reduction have operated extensively (both in field of view and elsewhere in thin section) as indicated by very fine (50-100 μm) grain size of surrounding quartzofeldspathic component. C-S fabric elsewhere in thin section clearly shows dextral shear sense. Cut parallel with lineation (14°N), perpendicular to foliation (060°/38°E). South is to right. Base of image is 5.5 mm and parallel with main fabric. Crossed polars.

Figure 5.43



Figure 5.43 Granitic orthogneiss in Rupal side valley at outcrop #18. This type of granitic orthogneiss is ubiquitous to the Rupal-Chichi shear zone. Asymmetric fabric is marked by (1) biotite planes clearly forming S and C surfaces, and (2) thin 0.5-20 mm feldspar porphyroclasts with asymmetric tails. Foliation is $040^{\circ}/80^{\circ}W$ and stretching lineation plunges 50° towards 238° . Sense of displacement is NW side upwards and vergent towards NE (dextral shear).

Figure 5.44

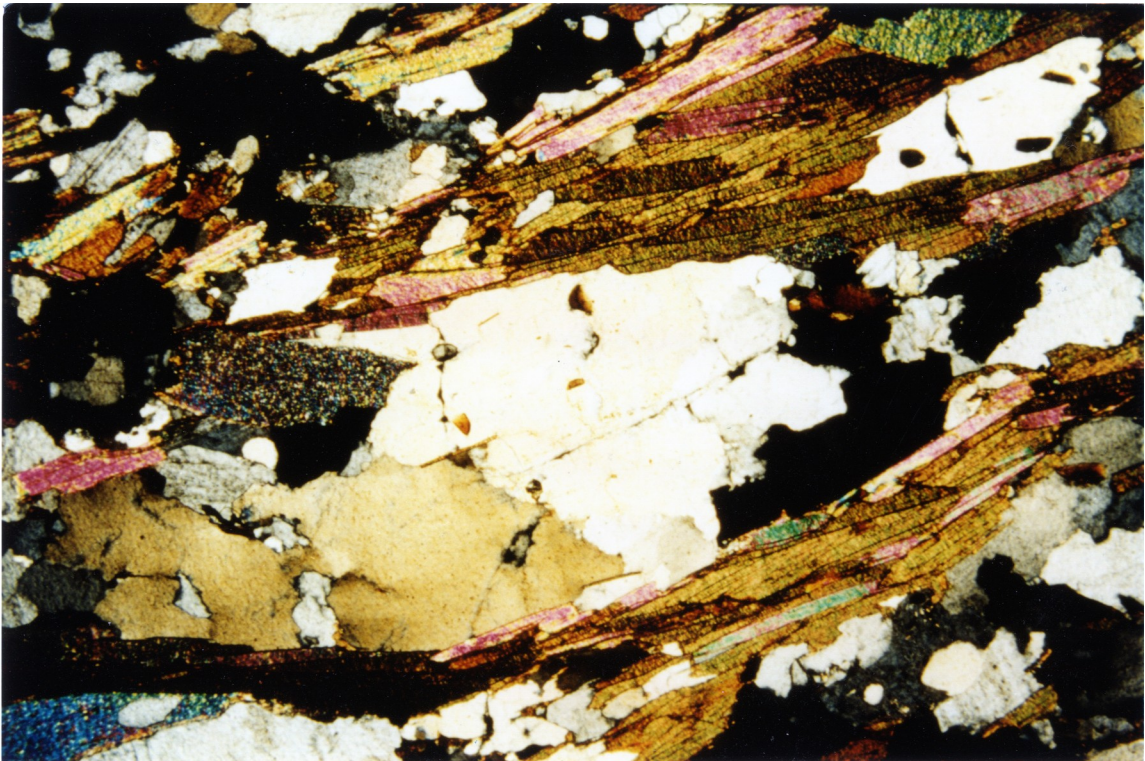


Figure 5.44 Optical photomicrograph of thin section 66/18D (cut from E6/6/18-IV, not shown), ~1 km NW of #18. Shows characteristic microstructure of RCSZ orthogneiss deformation conditions (note finer grained portion hence >2 mm feldspar porphyroclasts not shown). Sense of shear clearly dextral based upon sigmoidal feldspar porphyroclast tails; 600-1000 μm biotite surfaces define C and S surfaces (distinct in overall thin section). Note coarseness of grains and only very slight suturing of internal grain boundaries. Some recovery may have operated but lack of evidence for significant subgrain rotation recrystallisation within grain suggests less than 400°C temperature of deformation. Cut parallel with lineation ($50^\circ@238^\circ$), perpendicular to foliation ($040^\circ/80^\circ\text{W}$). South is to left. Base of image is 5.5 mm and parallel with main fabric. Crossed polars.

Figure 5.45

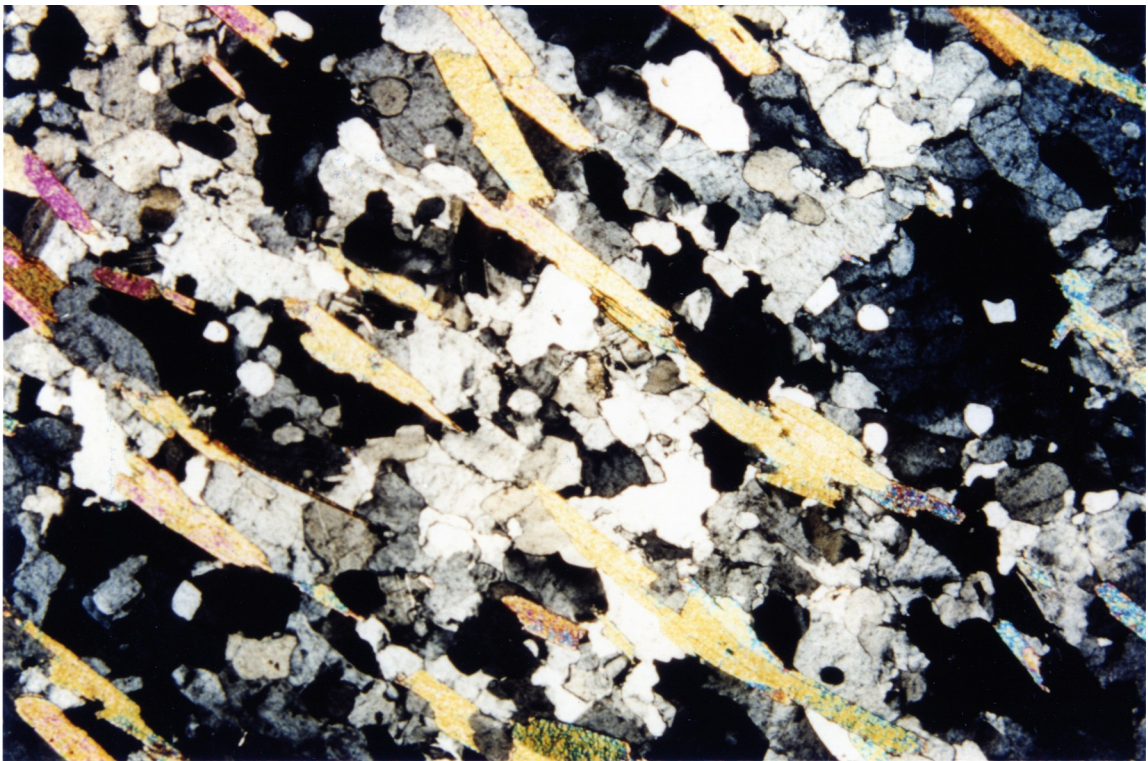


Figure 5.45 Optical photomicrograph of thin section cut from KC-9A, collected ~300 m north of outcrop #CC4, illustrates microstructure of granitic dyke cross-cutting main RCSZ granitic orthogneiss. Note lack of strain evidence in quartzofeldspathic portions; grains have even extinction and grain size distribution is small. Preferred lattice orientation of biotites is likely a product of super solidus strain. Sample from loose block not possible to orient. Base of image is 5.5 mm. Crossed polars.

Figure 5.46



Figure 5.46 View to NW of general area of #CC5 in southern Chichi Nallah. photo shows moderately WNW dipping sequence of metapelitic schists interlayered with quartzite, marble and amphibolite. Snow covered, tan-coloured hills in background at right of picture are granitic orthogneiss. Contact between granitic orthogneiss and metasedimentary sequences is immediately below snow covered top of ridge in foreground. This is ~500m from fan at base of picture. Metasedimentary sequences are fully concordant with the granitic orthogneiss (see text for discussion).

Figure 5.47



Figure 5.47 Photo showing tight folding in quartzite layers within metasedimentary sequences in general area of #CC5 (portion of outcrop shown in fig. 5.46). Hinge plunges 22° towards 223° , average local foliation: $023^\circ/71^\circ\text{W}$.

Figure 5.48



Figure 5.48 Photo showing isoclinal asymmetric folding in quartzite layers separating biotite schist (right) from granitic orthogneiss (far left) in general area of #49a. Hinge plunges 62° towards 343° , average local foliation: $152^\circ/58^\circ\text{E}$. Fold asymmetry indicates east limb of antiform, consistent with nearby observation.

Figure 5.49



Figure 5.49 Photo in vicinity of outcrop #54 - Mazeno Low Camp, showing moderately north-dipping compositionally layered gneiss (locally including metasediments). Stretching lineation is $36^\circ @ 317^\circ$.

Figure 5.50



Figure 5.50 Photo from #CR52 looking towards West Shagiri ridge, showing WSW trending metasedimentary and compositionally layered gneiss forming tight overturned steeply N-dipping synform, picked out by dark amphibolite layers. Fan in central portion is spilling down from Rupal left bank #1 Glacier. To left (west) of fan is granitic orthogneiss of #Sh2, to right are metasediments of #Sh1. Bottom of photo is ~3800m, ridge top in foreground is ~5500m. Note slight kinking in steeply N-dipping compositionally layered gneisses in background to far left of field of view.

Figure 5.51

Figure 5.51 (next page) Looking N to summit of Nanga Parbat (8143m), from #CR52 on Shaggin Glacier left bank. Nearly 5 km of relief is visible; long moraine ridge at foot of photo is Shagiri Glacier, and base of photo is ~3600m. Note ~50° NW dipping layer of black gneiss forming upper 400m of summit of Nanga Parbat. Below are thick sequences of granitic orthogneiss with local 100's metres thick leucogranite plutons. ~1.5 km thick pluton to left is characterised by "hooked boudin" xenolith. Extensive, cross-cutting pegmatitic dykes (part of 1.2 - 2.4 Ma suite) are just visible at bottom right. Lower regions of field of view contain ductile to brittle SE-vergent reverse faults, some of which show good evidence for later normal motion (see text for discussion).

Figure 5.51



Figure 5.51 (see previous page for caption).

Figure 5.52



Figure 5.52 Photo looking to NW to left bank of Toshain Glacier. Shows steeply W-dipping (and S-plunging lineation) fabric of compositionally layered gneisses interlayered with granitic orthogneiss in lower part of field of view decrease in dip sharply upwards. A thrust is inferred to separate lower rocks from moderately N-dipping compositionally layered gneisses interlayered with granitic orthogneiss above (see text for discussion).

Figure 5.53



Figure 5.53 Photo looking to NE to Nanga Parbat summit ridge from eastern Toshain Glacier. Local peaks on summit ridge average ~7000m. Nanga Parbat (8143m) is higher, and ~50° NW dipping biotite gneisses are hence clear. Extensive leucogranite (~1.5 km thick) is present on main Rupal Face. Valley in centre left of field of view is Mazeno Glacier valley. Join between Mazeno Glacier abandoned medial moraine and Toshain Glacier lateral moraine is ~4200m. Thrusts are interpreted on Mazeno Glacier valley left bank (1) in saddle partly obscured by shadow, and (2) in saddle (not visible, marked 5639m on map) between snow covered ridge in background and craggy ridge in centre.

Figure 5.54



Figure 5.54 L-tectonite granitic orthogneiss ~200m S of #CR52 on Shaggin Glacier left bank. This type of L-orthogneiss is ubiquitous to the SW Rupal area. Where foliation surfaces are clear, shear fabric is marked by (1) biotite planes forming S and C surfaces, and (2) 0.1-3.0 cm asymmetric feldspar porphyroclasts. Foliation is $031^{\circ}/70^{\circ}W$ with stretching lineation pitching 62° from south. Sense of displacement is top down to SW and sinistral.

Figure 5.55



Figure 5.55 Optical photomicrograph of thin section 69-28A (cut from E6/9/28-I sampled near #CR52). Shows characteristic microstructure of L-orthogneiss in SW Rupal. Sense of shear is sinistral, rarely visible at <10 mm width of view due to coarseness of fabric. Sigmoidal feldspar porphyroclasts and 100-400 μm biotite surfaces are main shear indicators. Note overall coarseness of grains. Although some compositional banding is present, quartzofeldspathic bands do not have ribbon-type appearance, and I suggest lattice preferred orientation of biotites is a relict of super-solidus flow, and principal deformation proceeded at <400°C. Cut parallel with lineation (50°-S pitch), perpendicular to foliation (037°/66°E). South is to left. Base of image is 5.5 mm and oblique to main fabric. Crossed polars.

Figure 5.56



Figure 5.56 Granitic orthogneiss on Mazeno Glacier Valley left bank at outcrop #21. Biotite planes mark S and C surfaces. Shear sense is also demonstrated by coarse (<2 cm) feldspar porphyroclasts with asymmetric tails. Foliation is $020^{\circ}/90^{\circ}W$ and stretching lineation plunges 50° towards 020° . Sense of displacement is E side upwards and vergent towards S (dextral shear).

Figure 5.57



Figure 5.57 Photo (looking due east) showing suite of NW dipping pegmatitic sheets ~500-1000 m north of #22, Sheets are discordant to local foliation but, interestingly, are parallel to foliation of country rock (gneiss) at #23, ~1 km across the glacier to the NW, and at Mazeno Pass. Glacier in foreground is ~5000 m. Float includes granitic orthogneiss and various members of compositionally layered gneisses. Green pinnitised cordierite in coarse (pegmatitic) granitoid float was seen in significant volumes, but not in outcrop.

Figure 5.58



Figure 5.58 Looking at east side of Mazeno Pass. Compositionally layered gneiss trending $050^{\circ}/80^{\circ}W$ is clear. Note lack of visibility of Mazeno Pass Pluton from only few 100 m from Pass. Compositionally layered gneisses are cut at high angle by fine grained leucogranite offshoots of Mazeno Pass Pluton (not visible in photo). Pass is 5358 m, top of outcrop to left is $\sim 5400m$.

Figure 5.59



Figure 5.59 View directly up steep West face of Mazeno Pass. Viewer is ~300 m below pass (snow covered lower spot to left of picture). Photo clearly shows Mazeno Pass Pluton main body and offshoots cross-cutting country rock (compositionally layered gneisses). Pluton continues for a further 100 m below and a few 100 m to both left and right of field of view.

Figure 5.61B



Figure 5.61B View (due W) from Airl Gali pass, looking (1) down Airl Gah, where >5 km of structural thickness of Jalhari granite is represented, (2) past Gashit fold where point of regional overturning of several km of MMT foot-, and hanging wall sequences is accommodated, (3) across Manogush Ridge (in shadow) where belt of porphyroclastic gneiss is present, (4) up into Nashkin Valley, where ~2600m of vertical relief, and >8 km of cover sequence is represented, and (5) to dark rocks of Kamila amphibolite that mark MMT hanging wall at very top of furthest ridge.

Figure 5.62



Figure 5.62 Looking NNW to outcrop of Gashit Fold, on right bank, and towards mouth, of Airl Gah Valley. In this outcrop, fold is within metasedimentary cover, ~1.5 km west of edge of Jalhari Granite. Fold accommodates regional overturning (eastward dip) of MMT footwall, and is inferred to be due to W-verging, E-dipping Airl-Gah/Diamir Shear Zone. North and East of this point, layering is predominantly E-dipping. South & West of this point, layering is predominantly W-dipping (note W-dipping cover rocks in background on far side of Bunar Gah). Hinge line plunges ~ 20°N

Figure 5.63



Figure 5.63 Strained portion of Jalhari granite within Airl-Gah Shear Zone, Diamir Valley: Note large variety of granitic gneiss locally housed. Sample is none the less representative of degree of variation observed throughout Jalhari Granite.

Figure 5.64



Figure 5.64 "Pancake biotite" portion of Jalhari granite within Airl-Gah Shear Zone, Airl Gah (~500 m W of #AR6). I infer large amounts of super solidus defamiation.

Figure 5.65

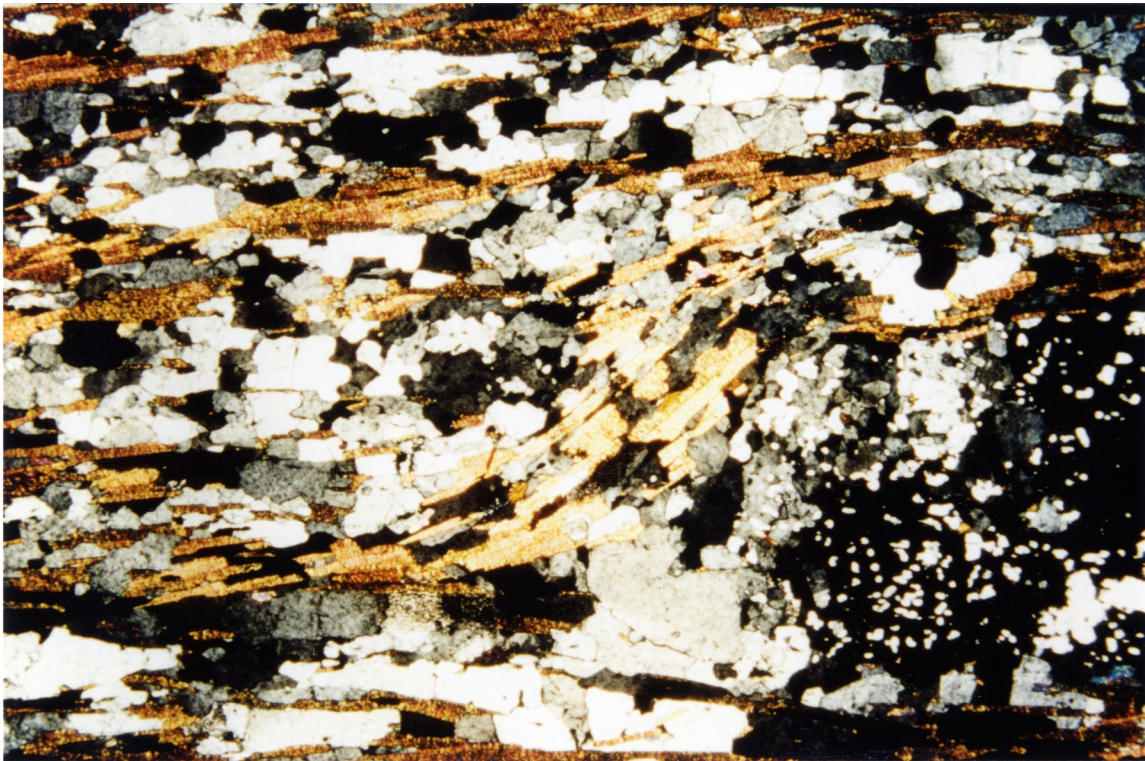


Figure 5.65 Optical photomicrograph of thin section 5-11G cut from NE95-11-VII (not shown). Note the partial development of polymineralic ribbons (see text for discussion). Shows characteristic microstructure of Jalhari granite in Diamir shear zone. Grain size is relatively fine (biotites $<300\ \mu\text{m}$, quartzofeldspathic grains $<400\ \mu\text{m}$). Biotite nicely picks out S and C surfaces. Sense of shear in this case is clearly dextral but note plunge of lineation ($50^\circ@350^\circ$) i.e., $>50\%$ of displacement (in present orientation) is W vergent. Cut parallel with lineation ($50^\circ@350^\circ$), perpendicular to foliation ($170^\circ/89^\circ\text{E}$). South is to left, west is to top. Base of image is 5.5 mm and parallel with main fabric. Crossed polars.